A Solution to the State Estimation Problem of Systems with Unknown Inputs

Hamidreza Bolandhemmat[1,*], Christopher Clark[2] and Farid Golnaraghi[3]

[1]*MicroPilot Inc. 72067 Road 8E, Sturgeon Rd. Stony Mountain, Manitoba, R0C 3A0, Canada;* [2]*Computer Science Program, Cal Poly State University, San Luis Obispo, CA, 93407, USA;* [3]*Mechatronics Systems Engineering, Simon Fraser University, Surrey, BC, Canada*

Received: September 26, 2011; Accepted: March 25, 2012; Revised: March 26, 2012

Abstract: A solution to the state estimation problem of systems with unmeasurable non-zero mean inputs/disturbances, which do not satisfy the disturbance decoupling conditions, is given using the Kalman filtering and Bayesian estimation theory. The proposed estimation algorithm, named Supervisory Kalman Filter (SKF), consists of a Kalman filter with an extra update step which is inspired by the particle filtering technique. The extra step, called supervisory layer, numerically solves the measurement equations for the portion of the state vector that cannot be estimated by the Kalman filter. First, it produces *N* randomly generated state vectors, the particles, which are distributed based on the Kalman filter's last updated estimate. Then, the estimated measurement vector associated with each particle is compared to the actual measurement vector to identify the particle's probability to be a solution. Finally, a so-called resampling stage is implemented to refine the particles with higher likelihoods. The effectiveness of the SKF is demonstrated by comparing its estimation performance with that of the standard Kalman Filter and the particle filter for a vehicle state estimation problem. The estimation results confirm that the SKF precisely estimates those states of the vehicle that cannot be estimated by either the Kalman filter or the particle filter, regardless of the unknown disturbances from the road. The filtering methodology offered in the article has a potential to improve performance of the systems presented in the patents WO2011115960, WO2010024751, US8073528, and US20110299730.

Keywords: Bayesian state estimation, disturbance decoupling conditions, inputs/disturbances, particle filtering, state estimation, systems with unknown kalman filtering, unscented kalman filtering.

I. INTRODUCTION

For many real estimation applications, some of the inputs to the system are inaccessible or the system is subjected to non-zero mean non-Gaussian disturbances. For example, consider aerodynamic parameters estimation of an aerial vehicle where some of the control surface deflections can not be measured or state estimation problem of a terrain vehicle suspension system which is disturbed by unknown non-zero mean non-Gaussian inputs from the road irregularities such as bumps.

In these cases, conventional estimation schemes such as Luenberger observer [1] or Kalman Filter (KF) [2, 3] fail to efficiently estimate a portion of the system states, since the fundamental assumption of having all the inputs (to the system) available for the model-based estimator is violated. A similar argument remains valid for Extended Kalman Filter (EKF) [4], Mixture Kalman Filter [5], and Unscented Kalman Filter (UKF) [6]. Particle Filters (PF) [7-9] can offer a more robust estimation performance compare to the Kalman-based filters by sampling and refining a number of hypothesized states. However, it is shown that for high-dimensional estimation practices, the PF capability is degraded significantly if it is not computationally too expensive to be implemented in real-time [10, 11].

One approach consists essentially of modeling and augmenting the unmeasurable input dynamics to the system model and to try to estimate the input states simultaneously [4, 11, 12]. This approach, however, increases dimension of the observer considerably which in turn, if still remains reasonable in terms of processing burden, may jeopardize Observability of the filter. Another approach is to utilize a suitable coordinate transformation to reduce order of the system and then to choose a reduced-order Luenberger observer gain to decouple the system states from the unmeasurable inputs [13-16]. The observer gain must also guarantee asymptotic stability of the estimation error. The required existence conditions for such a Luenberger observer (gain), referred to disturbance decoupling conditions, are extracted in [17-19]. One of the decoupling conditions needs the triple of the measurement matrix, state matrix and the unknown input matrix to not have an unstable invariant zero (i.e., no zero on or outside the unit circle). This condition, for some applications, is not satisfied [11].

This article presents a systematic estimation scheme for systems with unmeasurable non-zero mean non-Gaussian inputs/disturbances, which do not satisfy the disturbance decoupling conditions. The proposed algorithm, named Supervisory Kalman Filter (SKF), is a modified Kalman filter with an extra update layer inspired by the Bayesian estima-

*Address correspondence to this author at the MicroPilot Inc. 72067 Road 8E, Sturgeon Rd. Stony Mountain, Manitoba, R0C 3A0, Canada;
Tel: +1 204 344 5558; Fax: +1 204 344 5706; Ext: 226;
E-mail: hbolandhemmat@micropilot.com

2212-7976/12 $100.00+.00

tion theory and particle filtering technique. The extra layer, called the supervisory layer, numerically solves the measurement equations for the portion of the state vector that cannot be estimated by the Kalman filter due to the lack of input information. First, it produces N randomly-generated state vectors, the particles, which are distributed based on the Kalman filter's last updated probability distribution function (pdf) of the states. The other portion of the state vector that is accurately estimated by the Kalman filter remains unchanged in the particles. Then, each particle is assigned a weighting based on the relative distance between the corresponding estimated measurement vector and the actual measurement vector. Finally, particles with higher belief are selected and refined into a new particle set.

The filtering methodology offered in the article has a potential to improve performance of the systems presented in the patents WO2011115960, WO2010024751, US8073528, and US20110299730. Patent WO2011115960 [20] develops a control system for mobile robot path planning. The control system includes one or more models embedded in a Kalman filter to time-propagate all tracked objects states and multiple robot motion hypothesis. The predicted states are then fused with sensors measurement of spatial locations of at least one object and a priori map data and the robots information for object avoidance and trajectory planning. For outdoor applications where the robots can be exposed to unknown non-zero mean disturbances from an uneven terrain, the Kalman filter fails to estimate all or a portion of states of the robots. The proposed filter in the article, SKF, may be deployed to provide accurate estimates of the robots states in the presence of input uncertainties. The SKF can be also considered as an effective candidate for the tracking filter of the collision avoidance system developed in WO2010024751 [21].

In patent US8073528 [22], a surgical tool tracking system is outlined which utilizes a filter to generate the sequence of states of corrected kinematics information for the robotic instrument. The filter takes advantage of position information provided by a local camera system to correct the position information from an embedded robot kinematic model. Processing images of the cameras video frames are computationally extensive and using the SKF can help to effectively reduce the processor computational burden without compromising the estimation performance. The same argument remains valid for the patent US20110299730 [23].

Next section describes the estimation problem from a mathematical point of view. Section III develops structure of the SKF for linear systems with unknown inputs. Section IV is devoted to demonstration of the proposed filter performance in a benchmarked state estimation problem with unknown non-zero mean disturbances. The SKF is applied for the state estimation of a test vehicle suspension system, a Cadillac SRX 2005, which is driven on a road with a bump. Both off-line computer simulations and real-time estimation results are presented, and effectiveness of the SKF is confirmed through comparing its estimates with that of the KF, UKF and PF. Finally, section VII concludes the manuscript.

II. PROBLEM DESCRIPTION

Consider a dynamical system modeled by the following linear difference equation:

$$x_{k+1} = \Phi_k x_k + G u_k + E_d u_{d_k} + L w_k \; ; \; E[u_{d_k}] \neq 0, \; E[w_k] = 0. \tag{1}$$

In Eq. (1), the subscript k refers to the time-step, $x \in R^n$ is the state vector, $u \in R^m$ is the input vector containing m-known deterministic control inputs to the system, $u_d \in R^q$ is the q-dimensional unknown input vector of non-zero mean non-Gaussian disturbances, and also those control inputs which are inaccessible, and finally $w_k \in R^n$, process noise, is a zero-mean Gaussian white sequence with a power spectral density (covariance) of Q_k representing the uncertainties associated with the analytical model.

The measurement system is modeled as a linear combination of the states:

$$z_k = H_k x_k + v_k \; ; \; E[v_k] = 0. \tag{2}$$

In the measurement model, Eq. (2), $z \in R^p$ is the measurement vector, and $v_k \in R^p$ is the Gaussian white measurement noise with a power spectral density of R_k. It is assumed that the matrix pair (H_k, Φ_k) is observable (i.e., has full rank). Also, the following initial conditions are given:

$$\hat{x}_0^- = E[x_0]$$
$$P_0^- = E[(x - \hat{x}_0^-)(x - \hat{x}_0^-)^T]. \tag{3}$$

The problem consists of designing an estimator to asymptotically estimate the state vector x_k over time with no knowledge of the input vector u_d.

In the absence of u_d, the KF is the optimal solution to the above estimation problem [2, 4, 10]. However, when the non-zero mean unknown input u_d is acting on the system, the KF theory is violated since the estimation errors dynamic becomes u_d-dependent:

$$e_{k+1} = (\Phi_k - \Phi_k \bar{K} H_k) e_k + E_d u_{d_k} \; ; \; E[u_{d_k}] \neq 0 \tag{4}$$

Where e is the estimation error vector and $\bar{K}$ is the steady-state Kalman gain. If KF is implemented for state estimation of such a system, as Eq. (4) confirms, some of the states are not estimated precisely. Suppose that the estimation quality associated with $n_1 < n$ states of the state vector x_k becomes unacceptable in that the corresponding estimation error is biased and is not in agreement with the covariance bounds calculated by the KF. This is determined by analyzing Eq. (4) and/or computer simulation results.

For instance, the UKF estimation errors of the absolute vertical position of the test vehicle's Center of Gravity (CG) are plotted in Fig. (**1**) [11]. The results are obtained by using Monte Carlo simulations. It is shown that the estimation er-

$$E[\hat{x}^{+}_{1_{k,i}}(j)] = mean[p(x_k(j)\,|\,z_k)] = \hat{x}^{+}_{1_k}(j);\ i = 1,...,N, \quad (10)$$

$$\frac{1}{N}\sum_{i=1}^{N}(\hat{x}^{+}_{1_{k,i}}(j) - \hat{x}^{+}_{1_k}(j))(\hat{x}^{+}_{1_{k,i}}(j) - \hat{x}^{+}_{1_k}(j)) = \alpha \times cov[p(x_k(j)\,|\,z_k)] = \alpha P^{+}_{k}(j,j), \quad (11)$$

Where $\hat{x}^{+}_{k}$ and P^{+}_{k} are given by Eqs. (6) and (7), respectively. Also, α is a design parameter which is selected so that the particles are spread throughout variation ranges of the first n_1 state. It guarantees that the randomly generated particles are widely spread throughout the state space. In the other word, the bigger the proportion coefficient α be, the wider the area of the state space that the random particles are chosen from is. Since the x_2 portion of the state vector is accurately estimated by the KF, the remaining n_2 element of each particle, $\hat{x}^{+}_{2_{k,i}}(\ell)$'s $(\ell = 1,...,n_2)$, are set equal to the latest KF estimate $\hat{x}^{+}_{2_k}$:

$$\hat{x}^{+}_{2_{k,i}}(\ell) = \hat{x}^{+}_{2_k}(\ell);\ i = 1,...,N. \quad (12)$$

In the next step, particles which might be a possible solution are identified. This is achieved by evaluating relative distances between the actual measurement, z_k, and estimated measurements associated with the particles, i.e., $H_k\hat{x}^{+}_{k,i}$'s. The closer the estimated measurement to the actual measurement is, the higher the weighting is assigned to the corresponding particle. Given the probabilistic properties of the measurement noise, such a weighting can be calculated as follows:

$$q^{k}_{i} = p[v_k = (z_k - H_k\hat{x}^{+}_{k,i})];\ i = 1,...,N. \quad (13)$$

Next, particles with higher likelihoods q_i are selected to create a new set of N refined particle $\hat{x}^{+r}_{k,i}$ $(i = 1,2,...,N)$. Either of the resampling algorithms presented in [8, 9] can be utilized. A simple algorithm is given by the following two steps [8, 10]:

For $i = 1,2,...,N$,

Pick a random number ϑ from a uniform distribution on $[0,1]$.

Find ℓ such that, $\sum_{m=1}^{\ell-1} q^{k}_{m} < \vartheta$, but $\sum_{m=1}^{\ell} q^{k}_{m} > \vartheta$. Select the old particle $\hat{x}^{+}_{k,\ell}$ to be in the resampled particles set, i.e., $\hat{x}^{+r}_{k,i} = \hat{x}^{+}_{k,\ell}$.

A solution to the measurement equations, for the x_1 portion of the state vector, can then be approximated by calculating the expectation of the resampled particles:

$$\hat{x}^{+S}_{1_k}(j) = \frac{1}{N}\sum_{i=1}^{N}\hat{x}^{+r}_{1_{k,i}}(j)\ ;\ (j = 1,...,n_1). \quad (14)$$

Subsequently, the SKF estimate of the state vector at time $t = t_k$ is written as:

$$\hat{x}^{+S}_{k} = \begin{bmatrix} \hat{x}^{+S}_{1_k} \\ \hat{x}^{+}_{2_k} \end{bmatrix}, \quad (15)$$

Where, $\hat{x}^{+}_{2_k}$ is the outcome of the KF-type update, whereas $\hat{x}^{+S}_{1_k}$ is the output of the supervisory layer (PF-type update). If the resampling is performed efficiently, it can be shown that the ensemble pdf of the new particles $\hat{x}^{+r}_{k,i}$ converges to the conditional pdf $p(x_k\,|\,z_k)$ [10] ($\hat{x}^{+S}_{k}$ approximates the expectation $E[x_k\,|\,z_k]$), and therefore the error covariance associated with the SKF estimate $\hat{x}^{+S}_{k}$ can be approximated by P^{+}_{k}. Initialization process of the supervisory layer is summarized in block III of the SKF sequence block diagram in Fig. (**2**)). The current SKF estimate is now propagated to the next time frame and updated as outlines in sub-section B.

B. SKF Propagation and Update

After the initialization of the supervisory layer, either the latest SKF estimate $\hat{x}^{+S}_{k}$ or the refined particles $\hat{x}^{+r}_{k,i}$ can be propagated and updated (by the both update methods) to obtain the next estimates. In either case, since the estimation quality of the x_1 portion of the state vector is degraded due to the lack of information of the disturbance input u_d, estimates of this portion are propagated with the process noise w_k. This is to partially compensate for the effect of the unknown disturbance input. If the resampled particles are used[4], the first n_1 element of each particle is propagated as:

$$\hat{x}^{-}_{1_{k+1,i}}(j) = \varphi_k(j)\hat{x}^{+r}_{k,i} + g(j)u_k + L(j)w_{k,i};\ j = 1,...,n_1, \quad (16)$$

where $\varphi_k(j)$, $g(j)$, and $L(j)$ are the j^{th} rows of the state transition matrix Φ_k, the input matrix G, and the process noise matrix L, respectively. However, estimates of the x_2 portion are propagated without the noise, similar to the KF propagation method:

$$\hat{x}^{-}_{2_{k+1,i}}(\ell) = \varphi_k(\ell + n_1)\hat{x}^{+r}_{k,i} + g(\ell + n_1)u_k;\ \ell = 1,...,n_2. \quad (17)$$

[4] In the case of using the latest SKF estimate $\hat{x}^{+S}_{k}$, the estimate is propagated to the next time frame and updated upon receiving the new measurements by implementing Eqs. (6) and (7), i.e., the KF-type update method. Since, the x_1 portion estimate is not accurate, the supervisory layer steps, given by Equations (9) to (15), are then repeated.

In addition, the error covariance corresponding to each state estimate is propagated by including the system model uncertainty, i.e., covariance of the process noise. In the compact form, the propagated covariance matrix P_{k+1}^{-} is calculated by [4]:

$$P_{k+1}^{-} = \Phi_k P_k^{+} \Phi_k^T + LQ_k L^T , \quad (18)$$

Where P_k^{+} is the last updated covariance given by Eq. (7). Again, the process noise covariance term, $LQ_k L^T$, can be adjusted to compensate for the uncertainty contributed by the unknown disturbance input, $E_d E[u_{d_k} u_{d_k}^T] E_d^T$.

Upon receiving new measurements z_{k+1}, each particle is updated according to the KF update method, Equations (6), (7) and (8):

$$\begin{bmatrix} \hat{x}_{1_{k+1,i}}^{+} \\ \hat{x}_{2_{k+1,i}}^{+} \end{bmatrix} = \begin{bmatrix} \hat{x}_{1_{k+1,i}}^{-} \\ \hat{x}_{2_{k+1,i}}^{-} \end{bmatrix} + K_{k+1}(z_{k+1} - H_k \hat{x}_{k+1,i}^{-}), \; i = 1,...,N . \quad (19)$$

A summary of the SKF propagation and (KF-type) update procedure are given in block IV of the SKF block diagram (see Fig. (**2**)). Finally, the Supervisory layer (PF-type update) is implemented to solve for the x_1 portion.

C. Supervisory Layer

Since $\hat{x}_{1_{k+1,i}}^{+}$'s are not reliable, the x_1 portions of the updated particles are regenerated first. To do so, element $\hat{x}_{1_{k+1,i}}^{+}(j)$ $(j = 1,...,n_1)$ of each particle is replaced by a number picked up from a normal distribution with the mean value of $\hat{x}_{1_{k+1,i}}^{+}(j)$ itself and the covariance of $\alpha P_{k+1}^{+}(j,j)$ given by Eqs. (10) and (11) where P_{k+1}^{+} is the current updated error covariance which is calculated by Eq. (7). $\hat{x}_{2_{k+1,i}}^{+}$'s remain unchanged. After collecting the particles with higher belief, by using Eq. (13) and the resampling, the next SKF estimate is given by averaging the particles as follows:

$$\hat{x}_{k+1}^{+S} = \frac{1}{N} \sum_{i=1}^{N} \hat{x}_{k+1,i}^{+r} . \quad (20)$$

The above-mentioned steps in sub-sections B and C, i.e., propagation followed by the two update steps are recursively implemented until the supervisory layer function is terminated as a result of diminishing the disturbance input u_d ($E[u_d] = 0$). This is also sensed by the responsive sensor. After turning off the supervisory layer, the SKF is again a regular KF initiated by the latest SKF estimate, given by Eq. (20). The SKF algorithm is summarized in block diagram of Fig. (**2**). The same algorithm can be utilized for a nonlinear state estimation problem. However, instead of the KF as the preliminary estimator, a nonlinear estimator like the EKF or UKF is employed. Next section applies the SKF algorithm for state estimation of a Cadillac SRX test vehicle which is subjected to unknown non-zero mean disturbances from the road.

IV. KF PERFORMANCE DEMONSTRATION

Consider state estimation problem of a terrain vehicle, e.g., a Cadillac SRX test vehicle equipped with controllable dampers. Vehicle states are necessary for an active or a semi-active suspension control system, which is implemented to enhance ride comfort, road handling and stability of the vehicle. Figure **3** shows typical suspension control system architecture [24].

In the block diagram, the vehicle model is presented in the form of Eq. (1), where x is the state vector, u is the vector of control commands to the dampers, u_d is the vector of non-zero mean non-Gaussian disturbances from the road, and w is the vector of zero-mean Gaussian disturbances (also representing the model uncertainties). Vehicle motion of interest for this particular application consists of heave, roll, and pitch of the vehicle body, as well as bounce of the wheels. Therefore, a candidate for state vector x contains 16 states of the vehicle including relative displacement and velocity of each damper, and deflection and absolute (vertical) velocity of each wheel [11]. The vehicle model is verified and fine-tuned experimentally to match the desired modes of the vehicle dynamics (heave, roll, pitch and wheel bounces). Figure **4** depicts a 4-poster test facility where the fully instrumented test vehicle is excited by sweeping frequency (chirp) excitations of the base shakers.

z is the measurement vector in the block diagram of Fig. (**3**). The measurement system is usually a combination of accelerometers, gyroscopes and displacement sensors which are strategically distributed throughout the vehicle [11]. Information sent by the sensors is processed in the filtering unit. Output from the filtering unit are the vehicle states required by the control laws N. The controller assigns proper force or damping command to actuators for the current time-step.

Sensors are also modeled in the form of Eq. (2), by considering their noise characteristics [11]. For this practice, Analog Devices MEMS accelerometers ADXL202E and gyroscopes ADXRS401 [25] are utilized. The displacement sensors are non-contact rotary position sensors from Delphi [26]. Figures **5** & **6** show an accelerometer and a displacement sensor installed to measure acceleration of the wheel-hub and deflection across the shock, respectively.

Fig. (4). The Cadillac SRX test vehicle in the 4-posters test facility.

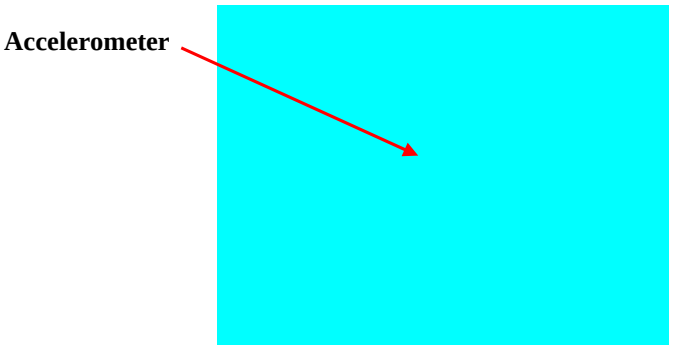

Fig. (5). An accelerometer mounted close to the wheel end of the shock.

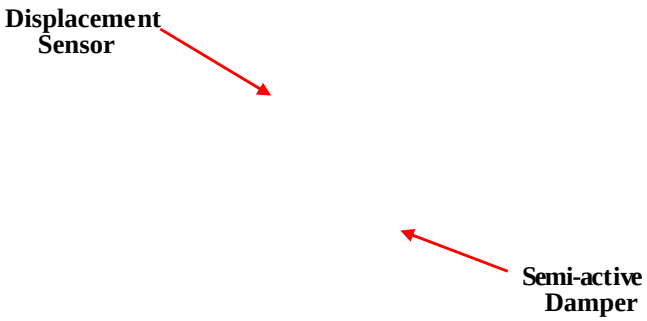

Fig. (6). The Cadillac SRX left front damper displacement sensor.

A software simulation and real-time processing platform developed on VC++ are used for off-line computer simulations and real-time implementation of the filters (KF, UKF, PF and SKF). The onboard computer is a Pentium 4 processor with 3.4GHz computational power (CPU) and 1GB RAM. The estimation algorithm is executed at a rate of 500Hz, which is the rate that accelerometers and gyros signal are sampled. Displacement sensors are sampled at approximately 200Hz.

The fully-instrumented test vehicle is driven on a selected segment of the University of Waterloo's ring road where there are two consecutive bumps. Figures **7** & **8** reflect the satellite picture of the ring road and the two bumps. The experiment is conducted at a speed of 40 km/hr.

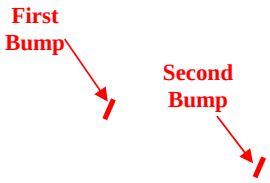

Fig. (7). Satellite picture of UW's ring road with two bumps.

Fig. (8). The first bump on the ring road.

By choosing proper sensor suite, i.e., an appropriate combination of sensors type and location, it is demonstrated that KF is capable of providing high quality estimates of the relative velocity and relative displacement states [11]. Figures **9** & **10** show typical KF estimation results for the relative velocity and displacement across the Left Front (LF) shock of the test vehicle over the first bump.

However, it is shown that the KF fails to estimate the absolute wheel-hub velocity states [11]. Figures **11** & **12** compare measured velocity of the LF wheel-hub with the KF estimate. As it is illustrated by the figures, as soon as the non-zero mean disturbance due to the bump is introduced to the front wheels (at approximately t = 3.7 sec), the KF estimate deviates from the actual signal and travels in the opposite direction.

Figure **13** plots the PF estimate of the Cadillac LF wheel-hub velocity [11] obtained by computer simulations. Simulations are performed with the same on board processor. It is assumed that the vehicle is driven over the same road and bumps. The PF is initiated by 10,000 randomly generated particles. Despite the high computational burden associated with the PF implementation, it is illustrated that it cannot provide accurate estimates of the wheel-hub velocity. The

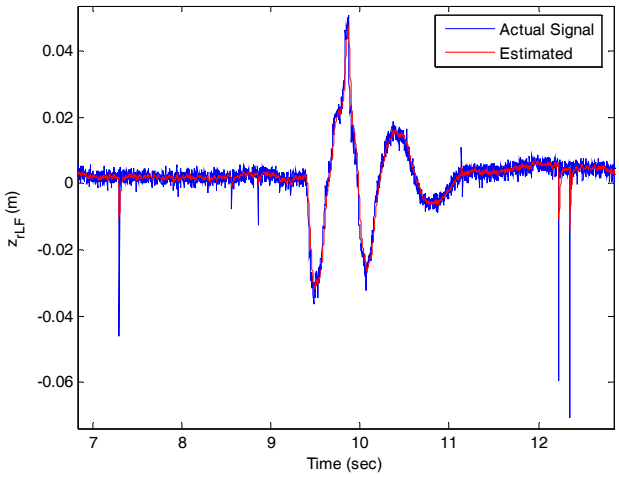

Fig. (9). The graph compares the actual relative displacement of the LF damper with its estimate zoomed on the first bump.

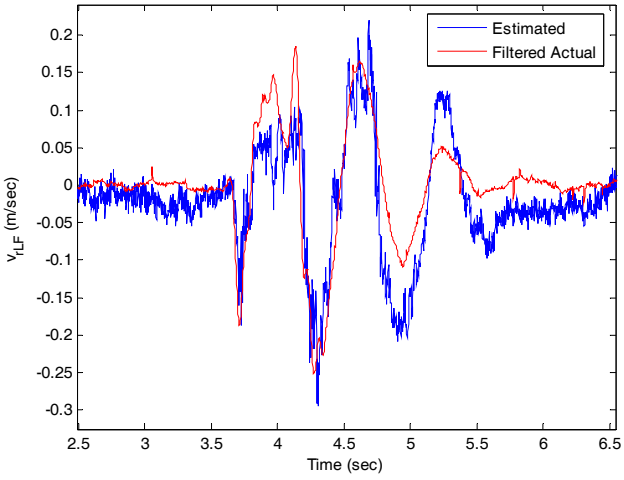

Fig. (10). The graph relates actual relative velocity across the LF damper and the real-time KF estimate on the first bump.

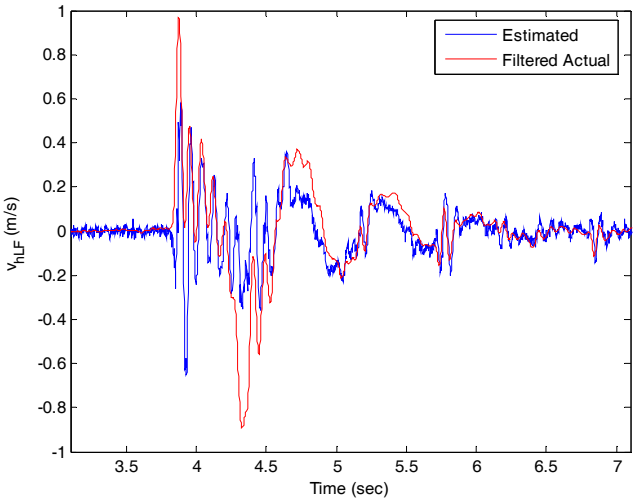

Fig. (11). The graph compares the actual velocity of the LF wheel-hub with its estimate on the first bump.

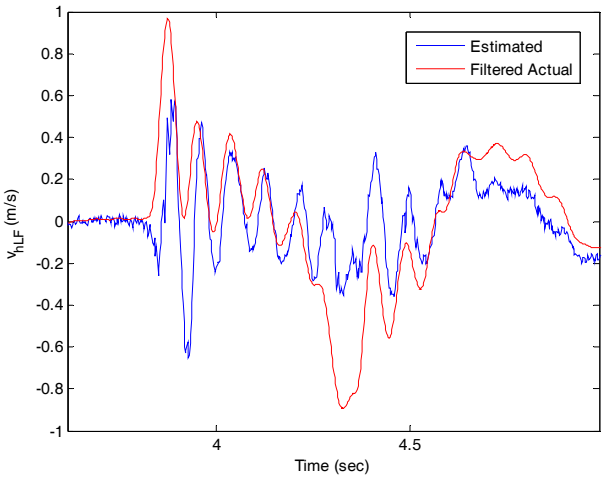

Fig. (12). The graph compares the actual velocity of the LF wheel-hub with its KF estimate zoomed right on the bump.

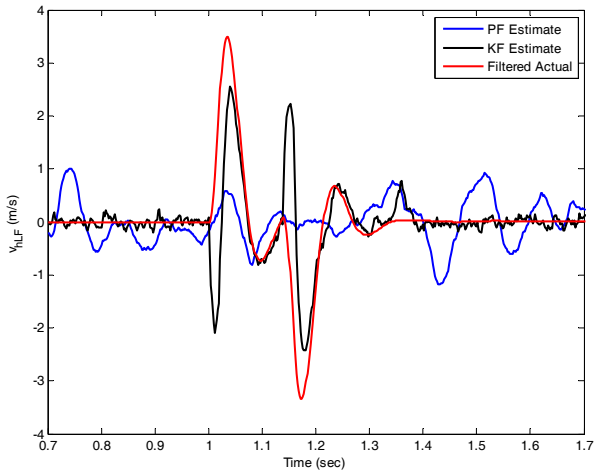

Fig. (13). Comparison of the PF and KF estimation performance for the absolute velocity of the LF wheel-hub.

KF estimation result for the same scenario is also given in the figure.

If the disturbance decoupling conditions are examined for the current estimation problem, it appears that regardless of the sensor configuration, the conditions are not satisfied [11].

Figure **14** demonstrates the SKF effectiveness in estimating the wheel-hub velocity state; the state that neither KF nor PF can accurately estimate. For the SKF implementation, x_1 includes the four wheel absolute velocity states and the rest of the states are partitioned in x_2 [11]. It is shown that the SKF estimate perfectly matches the actual velocity data during the period when the unknown non-zero mean disturbance is acting on the wheels. For the same period, the KF estimate does not remain reliable.

As illustrated in the figure, prior to the bump disturbance (before $t = 1$ sec), the SKF and the KF estimation results are

identical since the SKF works similar to the KF. As soon as the wheel-accelerometer triggers the supervisory layer, random particles, the green stars in Fig. (**14**), are generated based on the latest estimate (see Eqs. (9) and (10)). The magnifying coefficient α in Eq. (10) is selected to be $3\times n$, where $n=16$ is the dimension of the state vector. α should be big enough to assure that the particles are distributed all over the working space. Afterward, the particles are recursively processed by the three consecutive steps of the SKF algorithm until the accelerometers turns off the supervisory layer (end of the bump disturbance). Then, the SKF works again similar to a KF initialized by the latest SKF estimate.

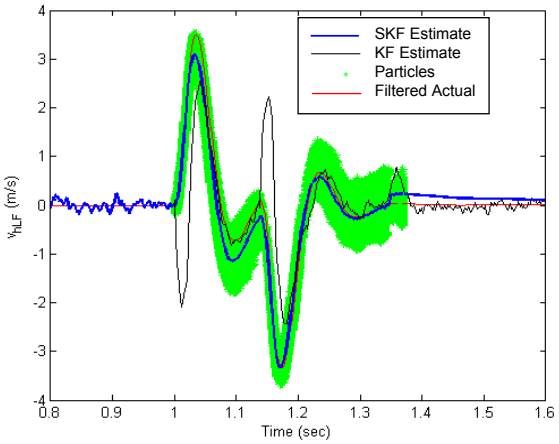

Fig. (14). Effectiveness of the SKF in estimating absolute vertical velocity of the LF wheel-hub.

The supervisory layer allows the SKF to explore wider regions of the state space than an ordinary KF to find the best estimates of the state vector. However, compared to the PF, the SKF spreads the particles more intelligently based on the updated estimates of a base filter such as a KF, EKF or UKF. In addition, since the search is accomplished only for the portion of the state vector which is not accurately provided by the base estimator[5], a fewer number of particles is required to guarantee the SKF convergence. This reduces the computational burden of the SKF significantly and makes it suitable for real-time applications. For instance, the accurate estimate for the wheel-hub velocity in Fig. (**11**) is obtained by a SKF which uses 200 particles[6]. With this number of particles, sample impoverishment [8-10], happens only after a few steps of the PF implementation.

The SKF estimate of the states in the x_2 portion, which are accurately estimated by the KF, is also maintained accurate. The estimation results are compared in Figs. (**15-17**). Figure **15** compares the SKF and KF estimates of the relative displacement across the LF damper. The comparison on the LF relative velocity state is given in Fig. (**16**). And finally, the tire deflection estimates are plotted in Fig. (**17**). Table **1** details the estimation error Root Mean Square (RMS) values for the two filters. Other than for the relative displacement estimate, which is slightly degraded, the SKF outperforms the KF in the presence of the unknown non-zero mean disturbance.

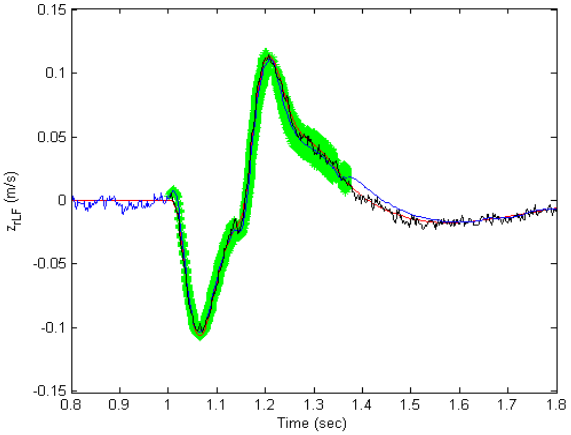

Fig. (15). Performance of the SKF in estimating the relative displacement of the LF damper.

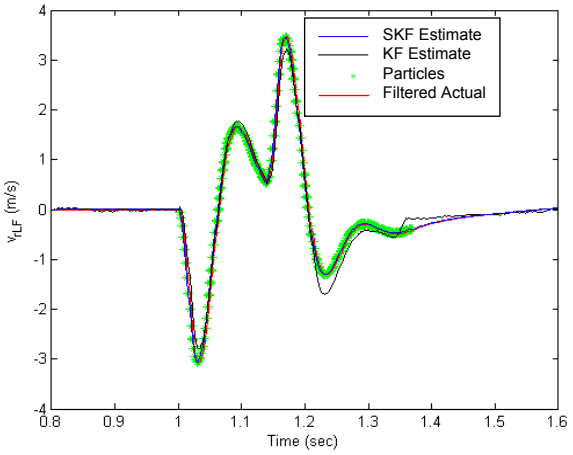

Fig. (16). Performance of the SKF in estimating the relative velocity across the LF shock.

Real-data estimation performance of the SKF is illustrated in Fig. (**18**). The estimation algorithm runs at a slower rate of 100 Hz with the same processor using the sensor data, logged during the real-time road experiments with the test vehicle. It uses 50 particles to initialize the supervisory layer. It is demonstrated that the SKF estimate of the LF wheel velocity remains reliable on the bump.

V. CURRENT & FUTURE DEVELOPMENTS

A solution has been given for the state estimation problem of systems with unmeasurable non-zero mean inputs/disturbances which do not satisfy the disturbance

[5] The Supervisory layer numerically solves a set of p stochastic equations for n_1 reduced unknowns whereas PF deals with $n > n_1$ unknowns.

[6] Even with only 20 particles, the experiments showed that the SKF estimation results remain sufficiently accurate.

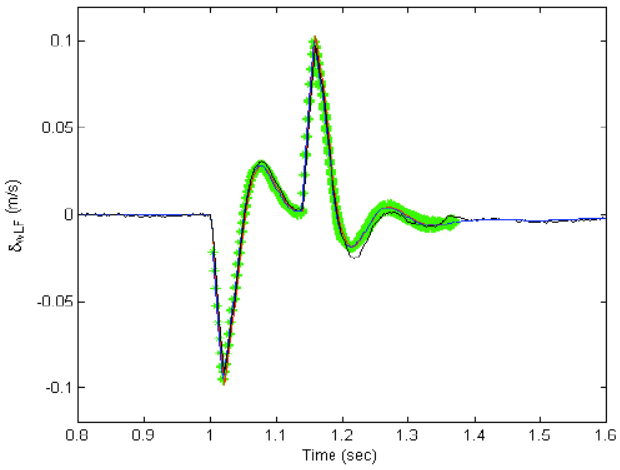

Fig. (17). Performance of the SKF in estimating the LF tire deflection.

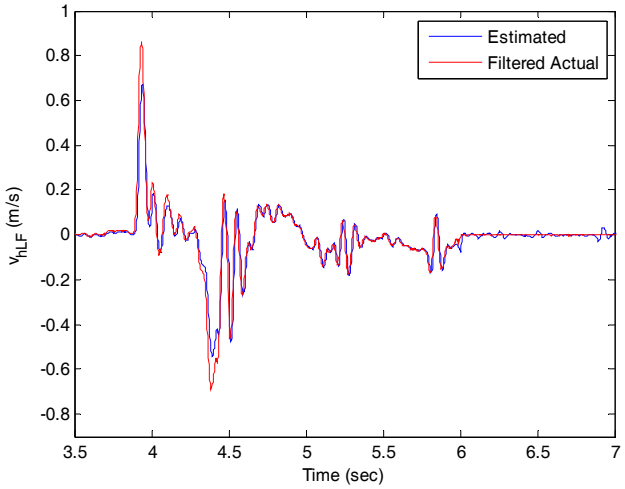

Fig. (18). The graph compares the actual vertical velocity of the LF wheel-hub with the SKF estimate on the first bump.

Table 1. Comparison of the Estimation Error RMS for the SKF and the KF Estimates of the LF Wheel/Suspension States.

State	KF Error	SKF Error
Relative displacement	0.0033	0.0039
Relative velocity	0.0962	0.0235
Absolute velocity	0.4851	0.0734
Tire deflection	0.0017	0.0008

decoupling conditions. Due to the lack of information of the non-zero mean disturbances, the conventional estimation techniques such as the Kalman filter fail to provide accurate estimates of the states. More robust estimators, such as the particle filter, also fail as a result of the system's high-dimensional structure. The proposed estimation algorithm, called Supervisory Kalman Filter (SKF), consists of a Kalman filter with an extra update step. The extra step, called supervisory layer, numerically solves the measurement equations at each time-step for the portion of the state vector that cannot be estimated by the Kalman filter.

Effectiveness of the SKF is demonstrated in estimating states of a Cadillac SRX suspension system which is subjected to unknown road disturbances. The estimation results confirm that the SKF precisely estimates states of the vehicle that cannot be estimated by either the Kalman filter or the particle filter in the presence of non-zero road bump disturbances. Although the filtering algorithm has been developed for linear systems, the same scheme can be utilized for nonlinear state estimation problems. However, instead of the Kalman filter as the preliminary estimator, a nonlinear estimator like the extended Kalman filter or unscented Kalman filter is employed.

Future development of the work involves mathematically proving the stability and convergence of the SKF. Also, derivation of the filter algorithm for a nonlinear case would be discussed in detail.

ACKNOWLEDGEMENTS

The authors would like to thank the Phoenix research team at the University of Waterloo. Also, the financial support, provided by Mechworks Systems Inc. and Ontario Centers of Excellence (OCE), is greatly appreciated.

CONFLICT OF INTEREST

The author has declared no conflict of interest.

REFERENCES

[1] Luenberger DG. Observer for multivariable systems. J IEEE Trans Automatic Contr 1996; AC-11: 190-7.
[2] Kalman RE. A new approach to linear filtering and prediction problems. ASME-J Basic Eng 1960; 82: 35-45.
[3] Kalman RE, Bucy RS. New results in linear filtering and prediction Theory. ASME-J Basic Eng 1961; 95-108.
[4] Gelb A, Kasper JF, Nash RA, Price CF, Sutherland AA. Applied Optimal Estimation. The M.I.T. Press, 1979.
[5] Chen R, Liu JS. Mixture Kalman filter. J Roy Statist Soc Ser B 2000; 62: 493-508.
[6] Julier S, Uhlmann JK. Unscented filtering and nonlinear estimation. Proceedings IEEE 2004; 92(3): 401-22.
[7] Salmond DJ, Gordon NJ, Smith AFM. Novel approach to nonlinear/non-Gaussian Bayesian state estimation. Proceeding IEEE F Radar Signal Process 1993; 140(2): 107-13.
[8] Ristic B, Arulampalan S, Gordon N. Beyond the Kalman Filter: Particle filters for tracking applications. Artech House Publishers, 2004.
[9] Arulampalam MS, Maskell S, Gordon N, Calpp T. A tutorial on particle filters for online nonlinear/non-Gaussian Bayesian tracking. J IEEE Trans Signal Proces 2002; 50(2): 174-88.
[10] Simon D. Optimal State Estimation. John Wiley & Sons Inc. Publication, 2006.
[11] Bolandhemmat H. Distributed Sensing and Observer Design for Vehicles State Estimation. Ph.D. dissertation, University of Waterloo, Waterloo, Canada, May 2009.
[12] Hostetter G, Meditch JS. Observing systems with unmeasurable inputs. J IEEE Trans Automat Contr 1973; 18: 307-8.
[13] Cumming SDG. Design of observers of reduced dynamics. Electronic Letters 1969; 5(10): 213-4.

[14] Wang S, Davison EJ, Dorato P. Observing the states of systems with unmeasurable disturbances. J IEEE Trans Automat Contr 1975; 20: 716-7.

[15] Bhattacharyya SP. Observer design for linear systems with unknown inputs. J IEEE Trans Automat Contr 1978; 23: 483-4.

[16] Bhattacharyya SP. Parameter invariant observers. J IEEE Trans Automat Contr 1980; 32: 1127-32.

[17] Kudva P, Viswanadham N, Ramakrishna A. Observers for linear systems with unknown inputs. J IEEE Trans T Automat Contr 1980; 25: 113-5.

[18] Hou M, Muller PC. Design of observers for linear systems with unknown inputs. J IEEE Trans Automat Contr 1992; 37: 871-4.

[19] Darouach M. On the novel approach to the design of unknown input observers J IEEE Trans Automat Contr 1994; 39(3): 698-9.

[20] Goulding, J.R. Temporal tracking robot control system. WO2011115960 (**2011**).

[21] Molander, S., Jonsson, J. Using image sensor and tracking filter time-to-go to avoid mid-air collisions. WO2010024751 (**2010**).

[22] Zhao, W., Hasser, C.J., Nowlin, W.C., Hoffman, B.D. Tool tracking systems, methods and computer products for image guided surgery. US8073528 (**2011**).

[23] Elinas, P., Perera, L.D.L., Nettleton, E., Durrant-Whyte, H. Vehicle localization in open-pit mining using GPS and monocular camera. US20110299730 (**2011**).

[24] Bolandhemmat H, Clark CM, Golnaraghi F. Development of systematic and practical methodology for the design of vehicles semi-active suspension control systems. J Veh Syst Dyn 2009; 48(5): 567-85.

[25] Analog Devices Specification Manual for ADXL202E Accelerometer and ADXRS401 Single Chip Rate Gyro. Available at: http://www.analog.com (Accessed on: August 2006).

[26] Delphi Non-Contact Rotary Position Sensor Data Sheet. Available at: http://www.wabashtech.com (Accessed on: March 2007).